Frontiers of Physics
https://doi.org/10.1007/s11467-019-0891-6
Front. Phys.
14(4), 42501 (2019)

RESEARCH ARTICLE

Transformation devices with optical nihility media and reduced realizations

Lin Xu[1,*,†], **Qian-Nan Wu**[2,*], **Yang-Yang Zhou**[3,*], **Huan-Yang Chen**[3,‡]

[1] *Key Laboratory of Opto-Electronic Information Acquisition and Manipulation of Ministry of Education & Institutes of Physical Science and Information Technology, Anhui University, Hefei 230601, China*
[2] *School of Science, North University of China, Taiyuan 030051, China*
[3] *Institute of Electromagnetics and Acoustics and Department of Electronic Science, Xiamen University, Xiamen 361005, China*
Corresponding authors. E-mail: †xuin@ahu.edu.cn, ‡kenyon@xmu.edu.cn
Received February 10, 2019; accepted March 5, 2019

Starting from optical nihility media (ONM), we design several intriguing devices with transformation optics method in two dimensions, such as a wave splitter, a concave lens, a field rotator, a concentrator, and an invisibility cloak. Though the extreme anisotropic property of ONM hinders the fabrication of these devices. We demonstrate that those devices could be effectively realized by simplified materials with Fabry–Pérot resonances (FPs) at discrete frequencies. Moreover, we propose a reduced version of simplified materials with FPs to construct a concentrator and a rotator, which is feasible in experimental fabrications. The simulations of total scattering cross-sections confirm their functionalities.

Keywords transformation optics, optical nihility media, Fabry–Pérot resonances

1 Introduction

In the past decade, researchers have found that the linear response parameters of materials can be equivalently considered as the curvature of the geometry property for electromagnetic (EM) wave propagation [1–4], which originates from the form invariance of Maxwell's equations under coordinate transformation and analogies to Einstein's theory of general relativity [5]. Based on such equivalent perspectives between material and geometry, transformation optics (TO) [6–12] was proposed as a theoretical method to design versatile optical devices and control the flow of electromagnetic waves, such as invisibility cloaks [1, 2, 13], carpet cloaks [14–16], concentrators [17–20], field rotators [21–23], EM wormholes [24] and so on. Moreover, the method of transformation optics was also introduced to manipulate other classical waves, such as acoustic waves [25], surface water waves [26, 27], elastic waves [28, 29] and thermal dynamics [30–33].

However, TO-based devices are usually required a complicated response of materials which is described by electromagnetic parameters (such as permittivity tensor ε and permeability tensor μ). Those materials are hardly founded in a native environment. Originally, the reduced invisibility cloak was achieved by split ring resonances (SSRs) in microwaves [13]. The structure of SRRs is a kind of typical metamaterials whose properties depend on local resonances of unit cells. The EM parameters of metamaterials can dramatically change near the resonant frequencies. After that, metamaterials were widely used to fabricate TO-based devices, such as carpet cloaks [15], field rotators [23] and so on.

More recently, photonic crystals for EM waves near at Dirac-like point was found to be like zero refractive index metamaterials [34], which can achieve invisibility effect as well. Such an effective zero refractive index stemmed from the collective behavior of ordered photonic crystal, which is a collective effect. In addition, some photonic crystal can also serve as an effective medium to construct TO-based concentrator [35].

Nihility media with $\varepsilon = \mu = 0$ [36] is a kind of metamaterials with a number of applications [37]. On the perspective of transformation optics, the definition of nihility media was generalized as transformation media derived from volumeless geometrical elements [38]. Later on, the structure of subwavelength apertures in metal was proposed to effectively achieve generalized nihility media, which is named "optic-null medium" [39, 40]. For simplification and unification, we would like to call such generalized nihility media as optical nihility media (ONM). The radiation cancellation effect and the hyperlensing effect were observed in the microwave at a single frequency [39]. However, the ONM is extreme anisotropic in EM parameters, which is quite hard to work at broadband frequencies.

In this paper, we firstly revisit ONM from extension coordinate transformation of volumeless geometry elements in Section 2. Then, we design several intriguing devices with ONM in Section 3, such as a wave splitter, a concave lens, a field rotator, a concentrator, and an invisibility cloak. Furthermore, we demonstrate that the functionalities of ONM can be effectively achieved by using simplified materials with Fabry–Pérot resonances (FPs) [18, 20] for

*L. Xu, Q. Wu, and Y. Zhou contributed equally to this work. arXiv: 1810.06155.

© Higher Education Press and Springer-Verlag GmbH Germany, part of Springer Nature 2019

transverse-electric(TE) EM waves. Moreover, we proposed the reduced realization of ONM by using the dielectric and thin metal plate in Section 4, which are used to construct a concentrator and a field rotator. The total scattering cross-sections demonstrate their functionalities in Section 5. We finally give a conclusion and discussion in Section 6.

2 The extension of volumeless geometry elements and the ONMs

Volumeless geometry elements in one dimensional (1D), two dimensional (2D) and three dimensional (3D) space are a point (P), a line (L) and a surface (S), as shown in the first column with purple color in Table 1, respectively. The additional counterparts and dashed lines (in blue) represent a small deviation Δx of those volumeless elements in one direction. When the deviation Δx is zero, the purple part and the blue part are the same to denote a volumeless geometry element. Starting from volumeless geometry elements as well as their deviation in virtual space (represented by x), for a point in Table 1 for example, its extension coordinate transformation in 1D is a line with length a, where its physical space is denoted by $x' = (a/\Delta x)x$. While its extension in 2D is a circular region, and in 3D a sphere, which are shown in the second row of Table 1. Those extended geometry elements in different dimensions are all called P-type ONM, which are similar to Ref. [38]. Dashed lines are mapped to extension paths with thin blue lines in P-type ONM. The extension coordinate transformation from one point to numerous points will result in singularities of P-type ONM in physical space. According to standard TO equation, $\varepsilon' = \Lambda^T \varepsilon \Lambda / \det(\Lambda)$, $\mu' = \Lambda^T \mu \Lambda / \det(\Lambda)$, where Λ is the Jacobian matrix of the extension coordinate transformation, the EM parameters of P-type ONM in 3D are $\varepsilon' = \mu' = 0$ [38]. Therefore, P-type ONM can be considered as zero-index materials. Moreover, the P-type ONM in 1D and 2D can be treated as a subspace of P-type ONM in 3D.

Table 1 The extension of volumeless geometry elements and the corresponding ONM. The first column is volumeless geometry elements. Dashed lines are mapped to extension paths with thin blue lines in ONM.

Volumeless elements	1D	2D	3D
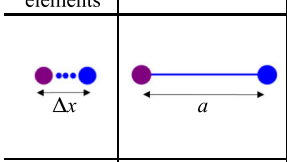		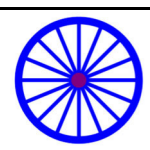	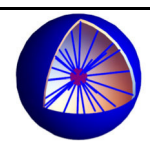
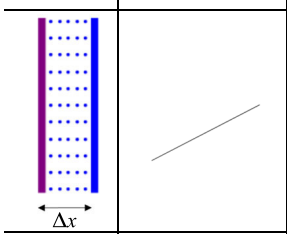		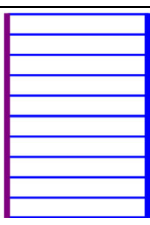	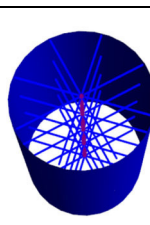
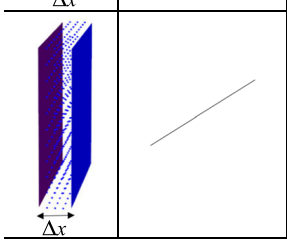			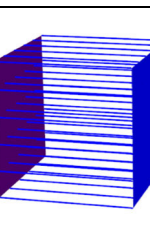

A line can be extended to a rectangular region in 2D or a cylinder in 3D as shown in the third row of Table 1. Its corresponding transformation media is called L-type ONM. The EM parameters of L-type ONM in 3D are $\varepsilon = \mu = \mathrm{diag}[1, 1, 0]$ [38]. The L-type ONM in 2D can be considered as a cross-section of L-type ONM in 3D.

In the fourth row of Table 1, the expansion of a plane in 3D virtual space is a cuboid volume. Its corresponding transformation media is called S-type ONM. The EM parameters of S-type ONM in 3D are $\varepsilon = \mu = \mathrm{diag}[\infty, 0, 0]$ [38].

There are two important properties of ONM. One is that light waves can only propagate along the extension paths. The second property is that a phase accumulation of light wave along the extension paths is zero. Although ONM in 3D is well studied in Ref. [38], we summarize them in a compact way here and show their properties respect to space dimensionality. In the following part, we will focus on L-type ONM and its reduced realization in 2D.

3 Several intriguing devices designed by L-type ONM

In 2D space, the extension of a line and L-type ONM can be used to design intriguing optical devices.

3.1 Splitter

Consider that a line in 2D extends to rectangular L-type ONM as shown in Fig. 1(a) on the left. Let us divide it with two black lines symmetrically such that the triangle with purple line and black lines is an equicrural triangle. Then we separate the original rectangular ONM into three parts as shown in Fig. 1(a) on the right. Such a configuration can serve as a wave splitter. The simulation with an incident Gaussian beam from the left demonstrates the splitting effect with L-type ONM, as shown in Fig. 1(b). All the simulation results in this paper are performed by the finite element solver COMSOL Multiphysics.

3.2 Concave lens

The shape of L-type ONM can be designed at will. In Fig. 1(c), the blue boundary of L-type ONM is set to be a

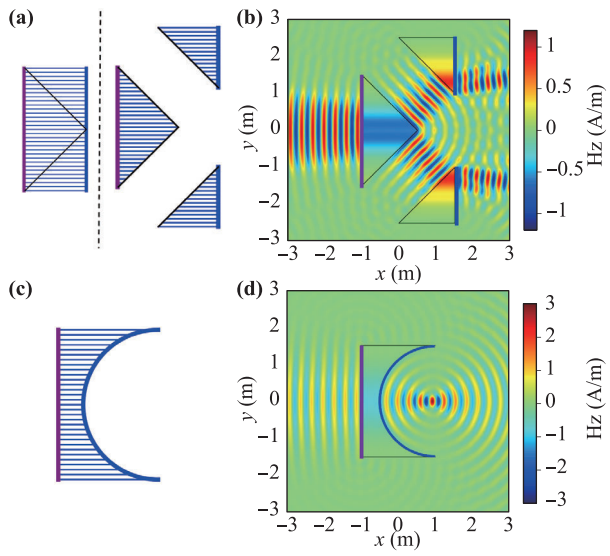

Fig. 1 **(a)** The design of a splitter with L-type ONM. **(b)** Hz field pattern of the splitter with L-type ONM. **(c)** The design of a concave lens with L-type ONM. **(d)** Hz field pattern of the concave lens with L-type ONM.

semi-circle. Then we obtain a concave lens designed by L-type ONM. Because there is no phase accumulation from the purple line to the blue semi-circle, the Gaussian beam focus at the center of semi-circle after passing through the concave lens as shown in Fig. 1(d).

3.3 Field rotator

In the previous design, the topology of ONM is the same as a point. In Fig. 2(a), we consider a volumeless element of a purple circle, it can be extended to the blue circle along curved thin lines, which forms a concentric ring region filled with ONM. The extension paths of each point in a volumeless element can be arbitrarily chosen as long as those paths do not intersect with each other. The topology of a circle is quite different from a point, it separates the whole 2D space into two disconnected regions. If we choose the extension path to be rotation linearly with the radius which is written as $\theta' = \theta + \Delta\theta \cdot (r - r_1)/(r_2 - r_1)$, we obtain L-type ONM in the concentric ring region. Furthermore, we compress the region with a purple circle on the left to the region with a blue circle under a coordinate transformation $r' = r \cdot r_1/r_2$. We then design a rotator with L-type ONM, whose rotation effect under a Gaussian beam is shown in Fig. 2(c).

3.4 Concentrator

Based on the above rotator, if we choose the extension path to be the radius, then we can design a circular concentrator with ONM as shown in Fig. 2(d). The property of such a concentrator has been systematically investigated in Ref. [18]. Here we demonstrate that such a concentrator can be viewed as a typical case made of L-type ONM. Moreover, we can also design another concentrator with a square shape as shown in Fig. 2(e).

3.5 Invisibility cloak

As shown in Fig. 2(b) on the left, four thick black extension paths are highlighted in the square concentrator. In principle, those four thick black lines are invisible because this square-shaped L-type ONM represents optical void. If we further extend them to four quadrangles bounded with black lines as shown in Fig. 2(b) on the right, we obtain an invisibility cloak with four invisible quadrangles. Its invisibility effect is demonstrated with an incident Gaussian beam in Fig. 2(f), where the four quadrangles are set to be metal.

4 Simplified materials with FPs and reduced version for L-type ONM

We have designed several intriguing devices with L-type ONM. How can we realize it? In the early days, the ONM was proposed and achieved by a compensated bilayer consist of positive and negative refractive index [38]. However, the negative refractive index medium is usually obtained by local resonances [41–43], whose functionalities are compromised by the absorption. As we have mentioned above the two important properties of ONM. The first one is that light flows along the extension path. The second one is that there is no phase accumulation along the extension path. To attain these two properties, we can reduce the second property to be the phase accumulation along the extension path is integer times of 2π. Such a reduction of phase accumulation is also referred to FPs [18]. Although the simplified material with FPs has already been discussed in Ref. [18]. In this section, we demonstrate that the L-type ONM can be effectively achieved by simplified materials with FPs. Moreover, we propose a reduced version of simplified material with FPs for experimental fabrications.

Let us consider a concrete example of a concentrator. In Fig. 2(d), the ideal concentrator with ONM can collect all energy impinging at the purple circle from an arbitrary direction to the inner region bounded with a blue circle. It is obvious that there is no phase accumulation of EM waves along the radial directions in the concentric ring region filled with L-type ONM. The L-type ONM can be replaced with simplified materials, as shown in Fig. 3(a). The main property of the simplified material parameters is the component along the radial direction of EM parameter tensors is infinity, while the components along other directions are continuous and finite. Therefore, EM waves can only propagate along the radial direction. The optical path along the radial direction in the simplified materials is $s_1 = \int_{r_1}^{r_2} \sqrt{\varepsilon} \cdot \mathrm{d}r$. At FPs, namely the frequency f

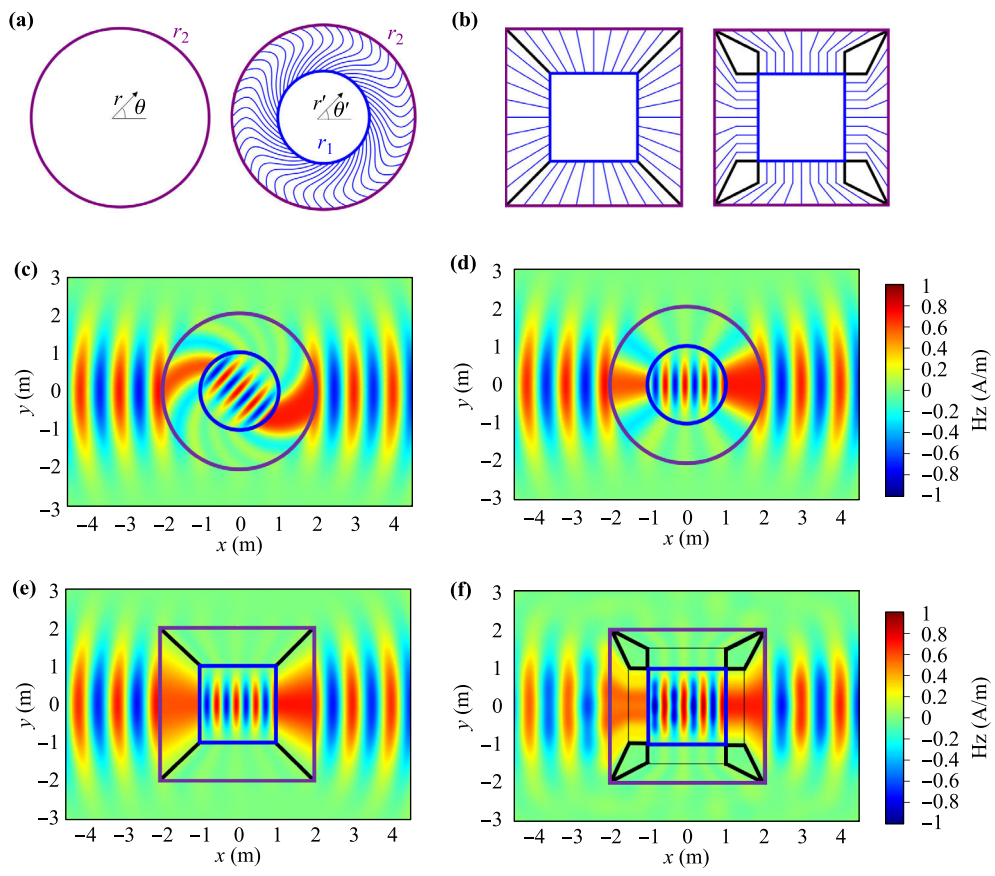

Fig. 2 **(a)** Extension of a circle along arbitrary paths. **(b)** The design of a square invisibility cloak with L-type ONM. **(c)** Hz field pattern of the field rotator with L-type ONM. **(d)** Hz field pattern of a circular concentrator with L-type ONM. **(e)** Hz field pattern of a square concentrator with L-type ONM. **(f)** Hz field pattern of a square invisibility cloak with L-type ONM. The invisible region is four quadrangles bounded with black lines.

satisfies $2s_1 = l_1 \cdot c/f$ with an integer l_1 and the speed of light in vacuum c, simplified materials act as L-type ONM. In Fig. 3(b), we show that the simplified materials can be effectively achieved by inserting plates made of metal (denoted with black lines) in a gradient dielectric profile with $\varepsilon = 4/r^2$, where transverse magnetic (TM) polarized EM waves cannot penetrate into them because of cut-off frequency of metal waveguide, but TE waves can. The metal is served as the perfect electric conductor (PEC) for the electric component of TE waves with arbitrary frequencies. If one wants to achieve the same reduced version for TM waves, the perfect magnetic conductor (PMC) is needed to guide TM waves with arbitrary frequencies. However, real PMC material is hard to find. Superconductors might be a candidate for the PMC material. As shown in Fig. 3(d), we plot the magnetic field along z-direction (Hz) for TE waves at FPs with $l_1 = 1$. It has been proved that the concentration effect is not perfect but still very good in such simplified materials [20]. Figure 3(e) shows the magnetic field for the effective gradient dielectric profiles inserted with 64 pieces of metal. Each unit cell is bounded with metal and its dielectric constant is ranging from 1 to 4. Since there is no cut-off frequency for TE waves in each metal waveguide, the effective medium theory is valid when the wavelength is much larger than the thickness of each unit cell. Due to the thickness of metallic plates and the simulation error, the working wavelength in Fig. 3(e) is shifted slightly from FPs with $l_1 = 1$ to 1.05 compared with Fig. 3(d).

In the effective gradient dielectric profiles with metallic plates, the dielectric constant changes continuously with radius. It is not easy to fabricate such materials in experiments. In a recent study, such a method is used to concentrate the energy of water surface waves, where effective continuous refractive index profiles can be tuned by changing the depth of the water surface [26]. Here in optics, we insert each unit cell with an equicrural triangle made of uniform material with its dielectric constant 4, as shown in the inset of Fig. 3(c). Therefore, we obtain a reduced version of simplified materials with a gear-shaped dielectric and metals. The effective refractive index can effectively change from 1 to 4 along the radial directions in each unit cell. However, it should not be exactly the same profile as Fig. 3(b). By numerical calculations, we find that there is concentration and invisibility effect nearby FPs with $l_1 = 1.2$ as shown in Fig. 3(f).

To further demonstrate simplified materials with FPs and a reduced version for L-type ONM, we also design a field rotator. The simplified materials are shown in Fig. 4(a). The shape of the bent extension path is obtained by the rotation mapping from that of the metal plates in Fig. 3(a), where the rotation angle is set to be $\Delta\theta = 0.5$ rad. The optical path along the bent extension path is $s_2 = \int_{r_1}^{r_2} \sqrt{\varepsilon} \cdot \mathrm{d}r$. At FPs, namely the frequency

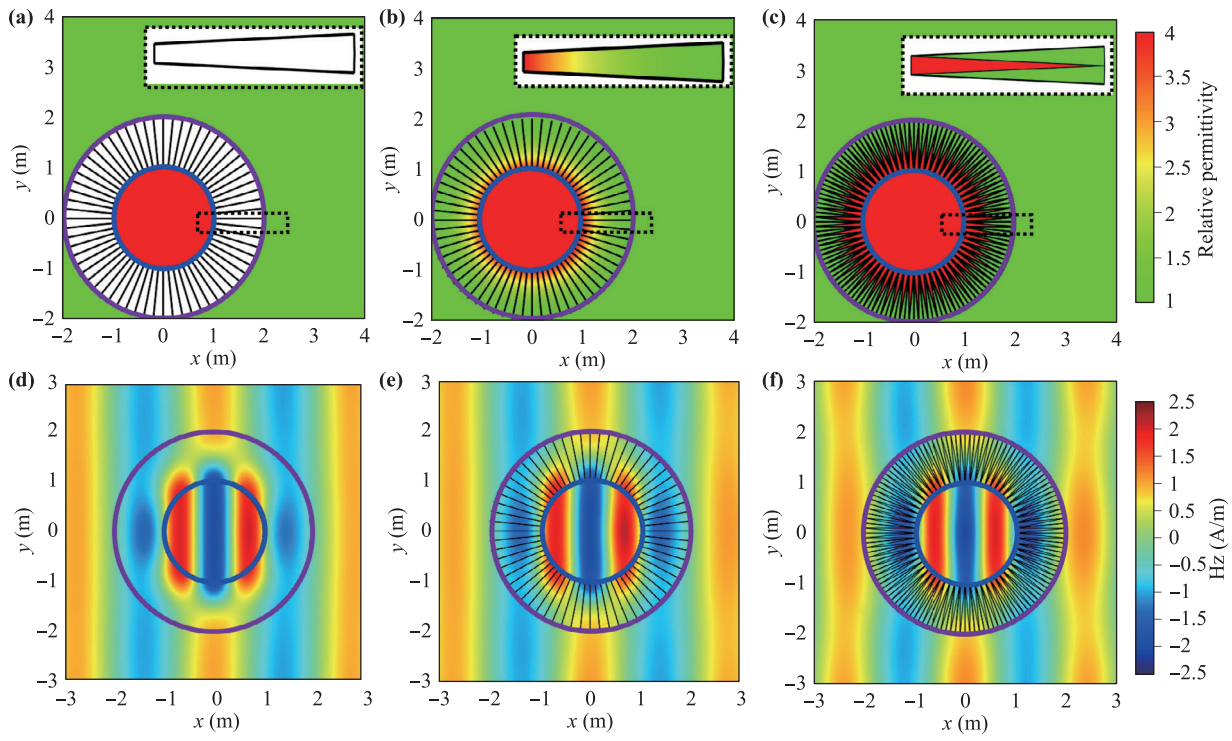

Fig. 3 **(a)** A concentrator of simplified material parameters with FPs. **(b)** A concentrator of effective gradient dielectric profiles with thin metal plates. **(c)** A concentrator of reduced realization with alternative dielectric and thin metal plates. **(d)** Hz field pattern of the concentrator of simplified material parameters with FPs. **(e)** Hz field pattern of the concentrator of effective gradient dielectric profiles with thin metal plates. **(f)** Hz field pattern of the concentrator of reduced realization with alternative dielectric and thin metal plates.

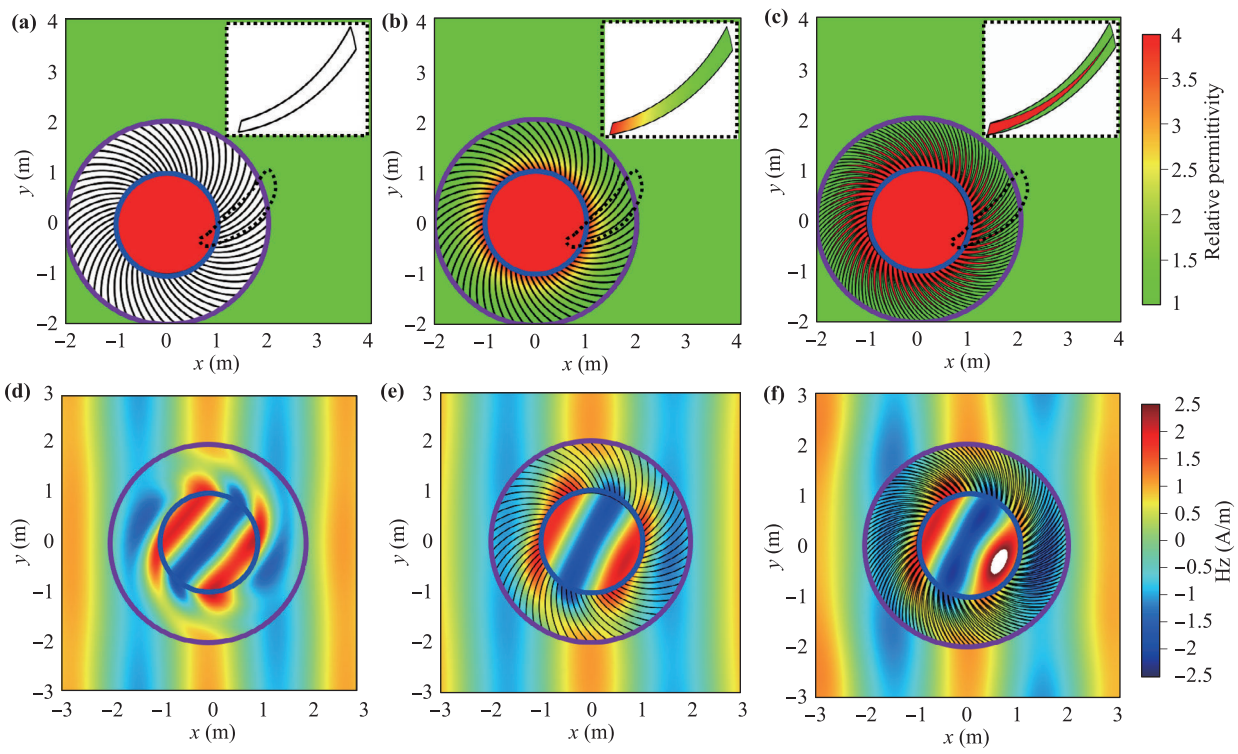

Fig. 4 **(a)** Field rotator of simplified materials with FPs. **(b)** Field rotator of effective gradient dielectric profiles with thin metal plates. **(c)** Field rotator of the reduced version with bent dielectric and thin metal plates. **(d)** Hz field pattern of field rotator of simplified materials with FPs. **(e)** Hz field pattern of field rotator of effective gradient dielectric profiles with thin metal plates. **(f)** Hz field pattern of field rotator of the reduced version with bending dielectric and thin metal plates.

f satisfies $2s_2 = l_2 \cdot c/f$ with an integer l_2, there should be the rotation effect. In the numerical calculations, the Hz field pattern of the simplified materials made of L-type ONM is shown in Fig. 4(d) at FPs with $l_2 = 1.05$. The configuration of effective gradient dielectric profiles with metallic plates of the rotator is shown in Fig. 4(b). There are 64 pieces inserted in gradient dielectric profiles. The unit cell is shown in the inset of Fig. 4(b). The related Hz field pattern is shown in Fig. 4(e) at FPs with $l_2 = 0.9$. The deviation of l_2 from 1 mainly results from the thickness of the unit cell, where the effective material parameters deviate a bit from the analytical form. By the rotation mapping, we obtain the reduced version made of bent gears and metals in Fig. 4(c) from that of Fig. 3(c). The Hz field pattern of the reduced version of the rotator is shown in Fig. 4(f) at FPs with $l_2 = 0.95$, which also exhibits a little of frequency shift.

5 Total scattering cross-sections

To further illustrate the property of reduced versions of L-type ONM. We integrate the scattering Hz in the far field as the total scattering cross-section. The integration radius is ten times the radius (10 m) of bare scatter with a dielectric constant 4. The total scattering cross-section of the concentrator with simplified materials is shown in a red curve in Fig. 5(a). The dips occur at FPs in the red curve, comparing to the dashed curve of bare scatter. Its effective concentrator is denoted with a blue curve which is similar to the red one. However, there is stronger scattering for the concentrator of the reduced version, where the dips with green curve shift a little, comparing to the previous two curves. It is because the effective material parameters are no longer the analytical form.

As for the rotators, the total scattering cross-sections for simplified materials, effective version, and reduced version are shown in Fig. 5(b) with red, blue and green curves, respectively. The shift of the blue curve from the red curve of rotators is quite large compared to that of the concentrator. This is because of the effective medium theory is not that exact due to the bending geometry. There is also deviation for the reduced version with the green curve, where the configuration is not only bending but also with gradient thickness, hence surely with only an approximate form. The reduced versions of FPs devices (denoted by the green curves) are made of finite pieces of metal and dielectric, comparing to infinite pieces in FPs devices (denoted by red curves). Therefore, the effective optical path of reduced version is shorter. Hence, the shift in frequency of green curves is always up compared to the red curves. Nevertheless, the similarity of those scattering cross-sections at FPs confirms that the concentration and rotation effect of L-type ONM can be effectively achieved by the reduced versions. There are also lots of working frequencies at FPs for the reduced versions.

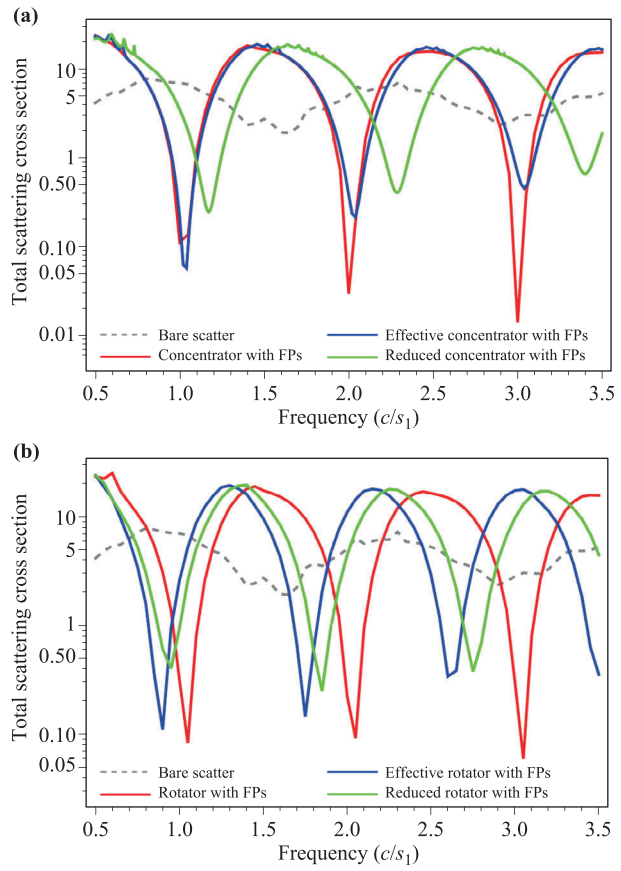

Fig. 5 Total scattering cross-sections for **(a)** concentrators and **(b)** rotators.

6 Conclusion and discussion

We revisit ONM from the extension coordinate transformations. Several intriguing devices, including a rotator and an invisibility cloak, are designed by L-type ONM. Since the fabrication of L-type ONM is quite challenging, we demonstrate that the property of ONM can be effectively achieved by the simplified materials with FPs. Although ONM and the simplified materials with FPs are not new concepts, their equivalence under phase reduction is revealed in this paper. Moreover, we propose reduced versions to construct a concentrator and a rotator, which only need dielectric and thin metal plates. The Hz field patterns and the total scattering cross-sections verify their functionalities. The reduced versions are neither based on metamaterials, nor on photonic crystals. It requires the phase accumulation along the extension paths, hence could bring in a further experimental realization of L-type ONM. The main advantage of the reduced versions is lower dissipation and much easier to fabricate. Such a reduced method can be generalized to manipulate the propagation of other classical waves, and extended to 3D ONM as well. However, reduced versions of 3D ONM with simplified materials for EM wave might be not easy

because of the coupling of different polarizations. Materials served as the PECs and PMCs, are hard to achieve for both polarizations. Nevertheless, we think such reduced 3D ONM might be achieved by metamaterials engineering with metals and superconductors.

Acknowledgements This work was supported by the National Natural Science Foundation of China for Excellent Young Scientists (Grant No. 61322504), the National Basic Research Program of China (Grant No. 2013CB035901), the Fundamental Research Funds for the Central Universities (Grant No. 20720170015), and the National Natural Science Foundation of China (Grants Nos. 51779224, 51579221, 51279180, 61705200, and 11874311).

References

1. U. Leonhardt, Optical conformal mapping, *Science* 312(5781), 1777 (2006)
2. J. B. Pendry, D. Schurig, and D. R. Smith, Controlling electromagnetic fields, *Science* 312(5781), 1780 (2006)
3. U. Leonhardt and T. G. Philbin, General relativity in electrical engineering, *New J. Phys.* 8(10), 247 (2006)
4. U. Leonhardt and T. Philbin, Geometry and Light: The Science of Invisibility, Dover Inc. Mineola, New York, 2010
5. A. Einstein, Die grundlage der allgemeinen relativitätstheorie, *Ann. Phys.* 354(7), 769 (1916)
6. H. Chen, C. T. Chan, and P. Sheng, Transformation optics and metamaterials, *Nat. Mater.* 9(5), 387 (2010)
7. A. V. Kildishev and V. M. Shalaev, Transformation optics and metamaterials, *Phys. Uspekhi* 54(1), 53 (2011)
8. B. Zhang, Electrodynamics of transformation-based invisibility cloaking, *Light Sci. Appl.* 1(10), e32 (2012)
9. P. Kinsler and M. W. McCall, The futures of transformations and metamaterials, *Photon. Nanostructures* 15, 10 (2015)
10. F. Sun, B. Zheng, H. Chen, W. Jiang, S. Guo, Y. Liu, Y. Ma, and S. He, Transformation Optics: From Classic Theory and Applications to its New Branches, *Laser Photon. Rev.* 11(6), 1700034 (2017)
11. M. McCall, J. Pendry, V. Galdi, Y. Lai, S. Horsley, J. Li, J. Zhu, R. Mitchell-Thomas, O. Quevedo-Teruel, P. Tassin, V. Ginis, E. Martini, G. Minatti, S. Maci, M. Ebrahimpouri, Y. Hao, P. Kinsler, J. Gratus, J. M. Lukens, A. M. Weiner, U. Leonhardt, I. I. Smolyaninov, V. N. Smolyaninova, R. T. Thompson, M. Wegener, M. Kadic, and S. A. Cummer, Roadmap on transformation optics, *J. Opt.* 20(6), 063001 (2018)
12. L. Xu and H. Chen, Conformal transformation optics, *Nat. Photon.* 9(1), 15 (2015)
13. D. Schurig, J. Mock, B. Justice, S. A. Cummer, J. B. Pendry, A. Starr, and D. Smith, Metamaterial electromagnetic cloak at microwave frequencies, *Science* 314(5801), 977 (2006)
14. J. Li and J. Pendry, Hiding under the carpet: A new strategy for cloaking, *Phys. Rev. Lett.* 101(20), 203901 (2008)
15. R. Liu, C. Ji, J. J. Mock, J. Y. Chin, T. J. Cui, and D. R. Smith, Broadband ground-plane cloak, *Science* 323(5912), 366 (2009)
16. H. F. Ma and T. J. Cui, Three-dimensional broadband ground-plane cloak made of metamaterials, *Nat. Commun.* 1(3), 21 (2010)
17. M. Rahm, D. Schurig, D. A. Roberts, S. A. Cummer, D. R. Smith, and J. B. Pendry, Design of electromagnetic cloaks and concentrators using form-invariant coordinate transformations of Maxwell's equations, *Photon. Nanostructures* 6(1), 87 (2008)
18. M. M. Sadeghi, S. Li, L. Xu, B. Hou, and H. Chen, Transformation optics with Fabry–Pérot resonances, *Sci. Rep.* 5(1), 8680 (2015)
19. P. Zhao, L. Xu, G. Cai, N. Liu, and H. Chen, A feasible approach to field concentrators of arbitrary shapes, *Front. Phys.* 13, 134205 (2018)
20. M. Y. Zhou, L. Xu, L. C. Zhang, J. Wu, Y. B. Li, and H. Y. Chen, Perfect invisibility concentrator with simplified material parameters, *Front. Phys.* 13(5), 134101 (2018)
21. H. Chen and C. Chan, Transformation media that rotate electromagnetic fields, *Appl. Phys. Lett.* 90(24), 241105 (2007)
22. H. Chen and C. Chan, Electromagnetic wave manipulation by layered systems using the transformation media concept, *Phys. Rev. B* 78(5), 054204 (2008)
23. H. Chen, B. Hou, S. Chen, X. Ao, W. Wen, and C. Chan, Design and experimental realization of a broadband transformation media field rotator at microwave frequencies, *Phys. Rev. Lett.* 102(18), 183903 (2009)
24. A. Greenleaf, Y. Kurylev, M. Lassas, and G. Uhlmann, Electromagnetic wormholes and virtual magnetic monopoles from metamaterials, *Phys. Rev. Lett.* 99(18), 183901 (2007)
25. H. Chen and C. T. Chan, Acoustic cloaking and transformation acoustics, *J. Phys. D* 43(11), 113001 (2010)
26. C. Li, L. Xu, L. Zhu, S. Zou, Q. H. Liu, Z. Wang, and H. Chen, Concentrators for water waves, *Phys. Rev. Lett.* 121(10), 104501 (2018)
27. H. Chen, J. Yang, J. Zi, and C. T. Chan, Transformation media for linear liquid surface waves, *EPL* 85(2), 24004 (2009)
28. M. Brun, S. Guenneau, and A. B. Movchan, Achieving control of in-plane elastic waves, *Appl. Phys. Lett.* 94(6), 061903 (2009)
29. A. Norris and A. Shuvalov, Elastic cloaking theory, *Wave Motion* 48(6), 525 (2011)
30. S. Narayana and Y. Sato, Heat flux manipulation with engineered thermal materials, *Phys. Rev. Lett.* 108(21), 214303 (2012)
31. H. Xu, X. Shi, F. Gao, H. Sun, and B. Zhang, Ultrathin three-dimensional thermal cloak, *Phys. Rev. Lett.* 112(5), 054301 (2014)

32. T. Han, X. Bai, D. Gao, J. T. Thong, B. Li, and C. W. Qiu, Experimental demonstration of a bilayer thermal cloak, *Phys. Rev. Lett.* 112(5), 054302 (2014)
33. C. Fan, Y. Gao, and J. Huang, Shaped graded materials with an apparent negative thermal conductivity, *Appl. Phys. Lett.* 92(25), 251907 (2008)
34. X. Huang, Y. Lai, Z. H. Hang, H. Zheng, and C. Chan, Dirac cones induced by accidental degeneracy in photonic crystals and zero-refractive-index materials, *Nat. Mater.* 10(8), 582 (2011)
35. J. Luo, Y. Yang, Z. Yao, W. Lu, B. Hou, Z. H. Hang, C. Chan, and Y. Lai, Ultratransparent media and transformation optics with shifted spatial dispersions, *Phys. Rev. Lett.* 117(22), 223901 (2016)
36. A. Lakhtakia, On perfect lenses and nihility, *Int. J. Infrared Millim. Waves* 23(3), 339 (2002)
37. I. Liberal and N. Engheta, Near-zero refractive index photonics, *Nat. Photon.* 11(3), 149 (2017)
38. W. Yan, M. Yan, and M. Qiu, Generalized nihility media from transformation optics, *J. Opt.* 13(2), 024005 (2011)
39. Q. He, S. Xiao, X. Li, and L. Zhou, Optic-null medium: Realization and applications, *Opt. Express* 21(23), 28948 (2013)
40. F. Sun and S. He, Surface transformation with homogenous optic-null medium, *Prog. Electromagnetics Res.* 151, 169 (2015)
41. J. B. Pendry, Negative refraction makes a perfect lens, *Phys. Rev. Lett.* 85(18), 3966 (2000)
42. D. R. Smith, W. J. Padilla, D. Vier, S. C. Nemat-Nasser, and S. Schultz, Composite medium with simultaneously negative permeability and permittivity, *Phys. Rev. Lett.* 84(18), 4184 (2000)
43. R. A. Shelby, D. R. Smith, and S. Schultz, Experimental verification of a negative index of refraction, *Science* 292(5514), 77 (2001)